Event-based Dynamic Optimization for Food Thermal Processing: High-Quality Food Production under Raw Material Variability

A.A. Alonso[1], J.L. Pitarch[2], L.T. Antelo[1], and C. Vilas[*,1]

[1]*Bioprocess Engineering Group. IIM-CSIC. c/ Eduardo Cabello,6. 36208 Vigo, Spain*
[2]*Instituto Univ. de Automática e Informática Industrial (ai2). Universitat Politècnica de València. Camino de Vera S/N, 46022, Valencia, Spain*

Abstract

Industrial canneries are subject to perturbations that may compromise food safety requirements. In such cases, plant operators typically increase the processing time, leading to undesirable large processing cycles and excessive quality degradation. In addition, differences among the items in a batch lead to variability in terms of quality and safety which, if not explicitly considered in the processing strategy, forces the use of conservative operation policies.

In this work, we present an event-based dynamic optimization approach that combines available plant measurements and mathematical model predictions to anticipate the effect of plant perturbations on food safety. A safety software sensor is build upon an on-line predictive simulation and a previous food-variability characterization such that, if any perturbation during the sterilization compromises food safety, a new processing strategy that optimizes a trade off among quality, uniformity and processing time is recomputed and implemented. Such multi-objective dynamic optimization problem under food product variability is efficiently addressed by taking advantage of the monotonicity and convexity properties of the food quality/safety dynamics.

Keywords:
Product variability; Model-based optimization; Food quality; Multi-objective optimization; Real-time software sensor; Microbial lethality sentinel

1 Introduction

Thermal processing is a time and energy demanding operation which employs around 70% of the total production time (Palacin and de Prada, 2019), and demands near 60% of the total energy consumed by a standard food processing factory (Peesel et al., 2016). In

*Corresponding author.
E-mail address: carlosvf@iim.csic.es

Preprint submitted to Food and Bioproducts Processing.
https://doi.org/10.1016/j.fbp.2021.02.013

addition, excessive processing may cause significant quality losses, in terms of nutrient or sensory indicators degradation, which has a direct impact on the consumer acceptance and, therefore, on the company turnover (Miri et al., 2008; Alonso et al., 2013). Optimization approaches have been widely used to minimize process duration (Chalabi et al., 1999; Simpson et al., 2004; Chen and Ramaswamy, 2004; Lespinard et al., 2012; Vilas et al., 2020), energy consumption (Peesel et al., 2016; Simpson et al., 2020) or quality degradation (Banga et al., 2001; Balsa-Canto et al., 2002; García et al., 2006; Simpson et al., 2008; Ansorena and Salvadori, 2011; Alonso et al., 2013; Ávila-Gaxiola et al., 2016). In these works, only one objective at a time is considered. Research focusing on optimizing several objectives simultaneously, i.e. multi-objective optimization problems, in the food industry has received less attention (Erdogdu and Balaban, 2003; Abakarov et al., 2009; Sendin et al., 2010; Madoumier et al., 2019). However, these works consider that all items to be processed are identical, so they do not address the problem of product variability.

Nevertheless, differences among the canned products to be processed in a batch usually result into different heat penetration rates, thus leading to differences in the values of quality and safety indicators reached by each of the items after sterilization. There exist different sources for such variability (Smout et al., 2000). For instance, spatial variability of the temperature inside the thermal processing unit (Cronin et al., 2000; Nicolaï et al., 2011) or differences from item to item in the quantity of food product, its compaction, and the quantity of packing liquid, among others. The characterization of such product variability in thermal processes for quality control purposes (e.g. color, texture or nutrients degradation) has received great attention in the last two decades (Nicolaï et al., 1998; Demir et al., 2003; Varga et al., 2000; Smout et al., 2000, 2003; Nicolaï et al., 2011). However, references to the design of optimal processing strategies in food products under variability are more scarce (Chalabi et al., 1999; Baucour et al., 2003; Cronin et al., 2007). In addition, most of these works focus just on the food product dynamics, disregarding retort dynamics which may lead to infeasible processing strategies in practice (Alonso et al., 2013). Besides, the usual way to handle product variability is based on Monte-Carlo simulations, with parameter values sampled from a probability distribution, performed at each step of the optimization procedure. This approach is not practical for real-time tasks, particularly when uncertainty is considered in more than one parameter. Therefore, efficient alternatives to solve the arising stochastic optimization problems are required to address this issue.

Another important aspect that must be considered is the presence, during the thermal processing cycles, of unexpected faults such as processing scheduling problems or deficiencies in the steam supply, particularly when resources are shared among the different equipment. These faults may cause that the optimal processing strategies cannot be fully tracked, compromising the safety of the food product and leading to the rejection or reprocessing of the batch (Alonso et al., 2013). Hazard analysis critical control point (HACCP) programs are designed to ensure safe production against such situations (Mortimore and

Wallace, 2013). However, those that do not integrate statistical process control (SPC) (Lim et al., 2014), either because there is no online monitoring and/or predictability of process variations, cope with these faults by increasing process time to avoid batch rejection, which usually results into an unnecessary degradation of product quality, uniformity as well as an expensive energy consumption increment. To avoid this limitation, advanced real-time control approaches capable of recomputing optimal processing strategies, using available plant measurements, have been proposed in the context of food thermal processing (Flores-Cerrillo and MacGregor, 2005; Banga et al., 2008; Kurtanjek, 2008; Alonso et al., 2013; Kondakci and Zhou, 2017). Nevertheless, again these approaches mainly focus on one objective or do not take into account the variability in the product properties.

In line with the recommendations for a good HACCP system, we analyze the main sources of variability in the sterilization of canned tuna that might compromise food safety, and we propose an event-based multi-objective dynamic optimization strategy that can detect and act against deviations in real time. Using the available plant measurements and the scheduled sterilization strategy, the proposed model-based safety sentinel is continuously monitoring (i.e. predicting) the microbial lethality to be reached at the end of the batch. In case a significant deviation in the selected safety requirement is detected, the event-based multi-objective dynamic optimization recomputes the processing strategy so that the effect of the perturbations on food quality, uniformity, and process time are minimized. Note that the approach easily integrates with SPC by explicitly considering food-product variability resulting from differences among items (e.g., the quantity of tuna in each tin can, its compaction, or the quantity of packing liquid, among others). Such variability translates into uncertainty on the thermal parameters, namely thermal diffusivity, and heat-transfer coefficients. The possible dependence of thermal parameters on the temperature, as well as measuring errors derived from instrument precision, are embedded within such uncertainty. However, uniform temperature within the sterilization unit is assumed in our case study. The multi-objective dynamic optimization problem (MODOP) under product variability is efficiently addressed by taking advantage of the convexity of food quality dynamics and the monotonicity of both food quality and safety dynamics with respect to the uncertain thermal parameters. This allows us to avoid the use of Monte-Carlo simulations which are computationally expensive. On the one hand, the monotonic behavior is exploited to define a polytopic bounding region, within the parameter variability, which allows us to ensure food safety by evaluating just the worst-case scenario. On the other hand, convexity is used in the context of the Jensen's inequality (Perlman, 1974) to maximize the average food quality by just considering one more scenario, in which we use the mean value of the thermal parameters. Both the sterilization unit and the food product mathematical models are used in the MODOP formulation to ensure that the optimal solutions can be implemented in the real plant.

The manuscript is structured as follows: first, we briefly describe the sterilization process on steam retorts, present the mathematical models representing the behavior of

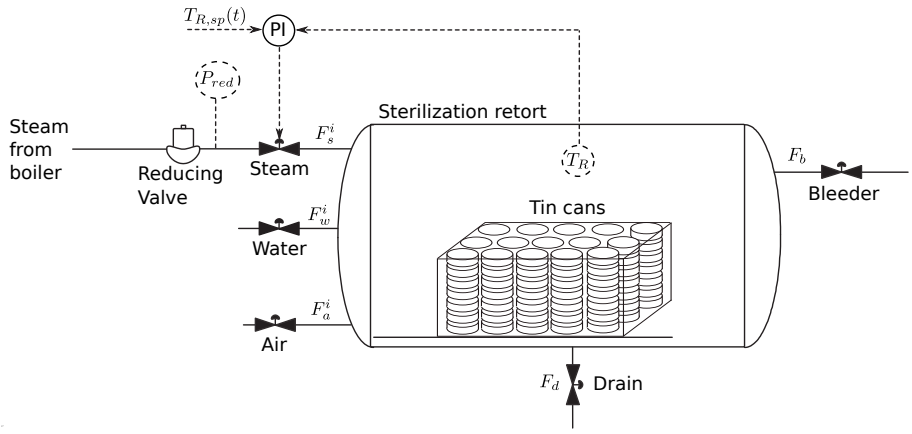

Figure 1: General scheme of the sterilization unit considered in this work. Available on-line measurements include the steam pressure after the reducing valve and the retort temperature.

the food product and sterilization unit, and describe the formulation and tools for solving the MODOP on-line. Then, we discuss the main outcomes of the work resulting from the application of the proposed event-based MODOP approach. Finally, the concluding remarks are presented.

2 Materials & methods

2.1 Sterilization unit description

The sterilization unit considered in this work consists of a steel vessel with a product storage grid box with rotary capacity and a fan to ensure uniform temperature inside the retort during the sterilization cycle (Figure 1). Steam generated in the boiler is subject to large pressure variations. Therefore, a reducing valve, that provides constant steam pressure, is installed before the retort steam valve. Then, the steam enters the retort and heats the packed food product. Temperature in the retort (T_R) and steam pressure after the reducing valve (P_{red}) are measured. In the first stage of the sterilization process (*venting stage*), air is removed from the retort by introducing steam, keeping the bleeder valve open. As a consequence, temperature in the retort rapidly increases in this stage. Then, during the *holding stage*, a PI controller, that actuates on the retort steam valve, is used to keep track of a given reference trajectory ($T_{R,sp}(t)$). At the end of this stage, water is introduced in the retort to rapidly cool down the food product and avoid further quality degradation, in the so-called *cooling stage*. Air is used to avoid large pressure drops during the cooling stage. Another valve is used to drain water from the vessel (either condensate or cooling water).

For the sake of completeness, the mathematical models of the packed product and sterilization unit will be briefly described in the following sections. Detailed model descriptions are provided in Alonso et al. (1997, 2013) and Vilas et al. (2018). The values

of the parameters are shown in Table 1.

Table 1: Values of the parameters included in the mathematical model of the sterilization unit, the food product and the different valves.

Parameter	Value	Units	Description
A	23.478	-	Antoine law parameter
B	-3984.8	-	Antoine law parameter
C	39.724	-	Antoine law parameter
V_R	0.3	m^3	Volume of the retort
A_R	3.1	m^2	Surface area of the retort metallic carcass
m_R	398.6	kg	Mass of the retort metallic carcass
$c_{p,R}$	500	$J\,kg^{-1}\,K^{-1}$	Specific heat of the retort metallic carcass
$c_{p,s}$	2200	$J\,kg^{-1}\,K^{-1}$	Steam specific heat
$c_{p,a}$	1010	$J\,kg^{-1}\,K^{-1}$	Air specific heat
$c_{p,w}$	4180	$J\,kg^{-1}\,K^{-1}$	Water specific heat
ρ_w	1000	kg/m^3	Water density
M_w	18.0	$kg\,kmol^{-1}$	Molecular weight of water
M_a	28.9	$kg\,kmol^{-1}$	Molecular weight of air
R	8314	$J\,kmol^{-1}\,K^{-1}$	Universal gas constant
λ	2260.9×10^3	$J\,kg^{-1}$	Steam condensation heat
θ	5.67×10^{-8}	$W\,m^{-2}\,K^{-4}$	Stefan-Boltzmann constant
ε	0.99	-	Thermal emissivity
$c_{v,s}$	5.2088	-	Steam valve parameter
$c_{v,a}$	5.0	-	Air valve parameter
$c_{v,b}$	6.8834	-	Bleeder valve parameter
K_p	0.1	-	PI controller parameter
τ_I	40	s	PI controller parameter
P_a^i	6.078×10^5	Pa	Air pressure in the inlet stream
P_w^i	6.078×10^5	Pa	Water pressure in the inlet stream
C_f	0.92	-	Gas valve parameter
G_f	1.0	-	Gas valve parameter
A_w, A_d	3.93×10^{-5}	$J\,kg^{-1}$	Water and drain valve parameter
P_{atm}	101 325	Pa	Atmospheric pressure
h_R	11.983	$W\,m^{-2}\,K^{-1}$	Heat transfer parameter retort/ambient
m_p	0.2	kg	Mass of the packed food product
ρ_p	1007	$kg\,m^{-3}$	Density of the packed food product
$c_{p,p}$	3653	$J\,kg^{-1}\,K^{-1}$	Specific heat of the packed food product
R_p	0.0418	m	Radius of the RO-200 tin can
L_p	0.03	m	Length of the RO-200 tin can
n_p	500	-	Number of RO-200 cans in the sterilizer
$z_{F,ref}$	10	K	Reference parameter for lethality
T_{ref}	394.25	K	Reference temperature for lethality
$z_{C,ref}$	14.93	K	Reference parameter for surface color
D_{ref}	8390.6	s	Reference parameter for surface color

2.2 Mathematical model of the food product

In this paper, we consider tuna packed in cylindrical RO-200 tin cans as the food product over which we illustrate the approach and extract conclusions, but note that other kinds of packages and/or canned food could be considered. The food product is mainly solid,

therefore, its temperature ($T_p(r, z, t)$) can be described by the following heat equation in cylindrical coordinates:

$$\frac{\partial T_p}{\partial t} = \alpha_p \left[\frac{\partial^2 T_p}{\partial z^2} + \frac{1}{r} \frac{\partial}{\partial r} \left(r \frac{\partial T_p}{\partial r} \right) \right]. \tag{1}$$

Robin boundary conditions are considered to describe the effect of the packing liquid on heat transmission on the top and bottom parts of the product:

$$\alpha_p \left. \frac{\partial T_p}{\partial z} \right|_{z=L} = h_t \left(T_R - T_p \big|_{z=L} \right), \qquad \alpha_p \left. \frac{\partial T_p}{\partial z} \right|_{z=0} = h_b \left(T_R - T_p \big|_{z=0} \right). \tag{2}$$

On the right boundary ($r = R$), the food product is in direct contact with the metal container. Therefore, Dirichlet conditions are considered. Besides, no-flux (symmetry) boundary conditions are used at $r = 0$:

$$T_p \big|_{r=R} = T_R.; \qquad \left. \frac{\partial T_p}{\partial r} \right|_{r=0} = 0. \tag{3}$$

In the above equations, α_p denotes the food product thermal diffusivity whereas h_t and h_b correspond with the heat transfer coefficients between the food product boundaries (top and bottom, respectively) and the retort, divided by the density (ρ_p) and specific heat ($c_{p,p}$) of the food product. The upper layer of packing liquid is thicker than the lower layer, therefore, h_t and h_b have different values. The different items to be processed in a batch are not identical. For instance, the quantity of tuna, its compaction or the quantity of packing liquid among other attributes differ from item to item. Therefore, parameters α_p, h_t and h_b vary from item to item. To characterize such variability, we assume that the values of the parameters belong to a normal distribution (Baucour et al., 2003; Cronin et al., 2007). Then, from extensive data collection through experimentation with instrumented cans, we were able to estimate the following mean values and standard deviations: $\mu_{\alpha_p} = 1.33 \times 10^{-7}$ m^2 s^{-1}, $\sigma_{\alpha_p} = 3.48 \times 10^{-9}$ m^2 s^{-1}, $\mu_{h_t} = 8.72 \times 10^{-5}$ m^2 s^{-1}, $\mu_{h_b} = 2.44 \times 10^{-4}$ m^2 s^{-1}, $\sigma_{h_t} = 9.68 \times 10^{-6}$ m^2 s^{-1}, $\sigma_{h_b} = 4.47 \times 10^{-5}$ m^2 s^{-1} (details omitted for brevity).

The application of classical numerical techniques, such as the Finite Element Method or the Finite Differences Method (Vande Wouwer et al., 2014), for solving Eqs. (1)- (3) results into a large number of ordinary differential equations, around 1000 in this case. This issue hampers the use of robust optimization techniques to this problem, in particular when solutions need to be obtained in real time. The *Proper Orthogonal Decomposition* method (Sirovich, 1987) is used to alleviate the computational burden. As a result, the following equivalent system consisting of 15 ordinary differential equations, is obtained:

$$\frac{\mathrm{d}s}{\mathrm{d}t} = \left(\alpha_p A_{\alpha_p} + h_t A_{h_t} + h_b A_{h_b} + h_r A_{h_r} \right) s + \left(h_t B_{h_t} + h_b B_{h_b} + h_r B_{h_r} \right) T_R. \tag{4}$$

where $s = [s_1, s_2, \ldots, s_{15}]$ are the modes of the POD method. A brief description of the derivation of Eq. (4) is provided in A. For more details about the method, the reader is referred to the literature (Sirovich, 1987; Vilas et al., 2018).

2.3 Mathematical model of the sterilization unit

2.3.1 Detailed mathematical model

The mathematical model describing the retort temperature has been developed in Alonso et al. (1997). For the sake of completeness, we will summarize here the final model equations. Evolution of steam, water and air mass in the retort is computed as:

$$\frac{\mathrm{d}m_s}{\mathrm{d}t} = F_s^i - x_s F_b - \chi, \tag{5}$$

$$\frac{\mathrm{d}m_w}{\mathrm{d}t} = F_w^i - F_d + \chi, \tag{6}$$

$$\frac{\mathrm{d}m_a}{\mathrm{d}t} = F_a^i - x_a F_b, \tag{7}$$

where, as shown in Figure 1, F_s^i, F_w^i and F_a^i are, respectively, the retort input flows of steam, water and air. F_b and F_d represent the bleeder and drain flows whereas x_s and x_a are the mass fractions of steam and air within the sterilization unit. The steam condensation flow (χ) is computed by finding the roots of the following equation:

$$\Psi(\chi) = m_s(\chi) - m_s^{eq}(\chi); \qquad m_s^{eq}(\chi) := \frac{P^{eq} V_v M_w}{R T_R}, \tag{8}$$

with V_v denoting the volume of retort that is not occupied by water or by the tin cans $V_v = V_R - \frac{m_w}{\rho_w} - n_p V_p$, where V_p is the volume of the RO-200 tin can. Equilibrium pressure (P^{eq}, in Pa) is computed from the retort temperature (T_R, in K) using Antoine's law $P^{eq} = \exp\left(A + \frac{B}{T_R - C}\right)$.

The temperature in the retort is described by the following equation, derived in Alonso et al. (1997) from an energy balance:

$$\left[m_s(c_{p,s} - R_s) + m_a(c_{p,a} - R_a) + m_w c_{p,w}\right] \frac{\mathrm{d}T_R}{\mathrm{d}t} =$$

$$F_s^i(c_{p,s}(T_s^i - T_R) + R_s T_R) + F_{a,i}(c_{p,a}(T_a^i - T_R) + R_a T_R) + \tag{9}$$

$$F_w^i c_{p,w}(T_w^i - T_R) - F_b T_R(x_s R_s + x_a R_a) + \lambda\chi - (Q_a + Q_p + Q_R),$$

where T_x^i with $x = s, w, a$ represents the temperature of the inlet streams whereas $R_s = R/M_w$ and $R_a = R/M_a$. Heat losses to the surrounding media (Q_a), heat absorbed by the retort metal carcass (Q_R), and heat absorbed by the food product (Q_p) are computed as:

$$Q_a = A_R\left(h_R\left(T_R - T_{amb}\right) + \theta\varepsilon\left(T_R^4 - T_{amb}^4\right)\right),$$

$$Q_R = m_R c_{p,R} \frac{\mathrm{d}T_R}{\mathrm{d}t},$$

$$Q_p = n_p m_p c_{p,p} \frac{\mathrm{d}T_{p,n}}{\mathrm{d}t}; \quad \text{with} \quad T_{p,n} = \frac{\int_{V_p} T_p(r,z,t)\mathrm{d}V_p}{V_p}.$$

Flows (in $\mathrm{kg\,s^{-1}}$) through the steam, air and bleeder valves are described by (Smith and Corripio, 1997):

$$F_x^i = 3.4 \times 10^{-8} c_{v,x} u_x C_f P_{red} \sqrt{Gf}\left(w_x - 0.148 w_x^3\right), \quad x = s, b, a. \tag{10}$$

$$w_x = \frac{1.63}{C_f}\sqrt{\frac{P_{in} - P_{out}}{P_{in}}},$$

with $u_x \in [0, 1]$ denoting the valve opening. For the steam valve, input and output pressures correspond, respectively, with the reducing valve pressure ($P_{in} = P_{red}$) and the retort pressure ($P_{out} = P_R$). For the air valve, $P_{in} = P_a^i$ and $P_{out} = P_R$. Finally, for the bleeder valve, $P_{in} = P_R$ and $P_{out} = P_{atm}$. Water and drain valves transport liquid so the flows through them can be computed as (Smith and Corripio, 1997):

$$F_d = A_d u_d \rho_w \sqrt{\frac{2\left(P_R - P_{atm}\right)}{\rho_w}}, \qquad F_w = A_w u_w \rho_w \sqrt{\frac{2\left(P_w^i - P_R\right)}{\rho_w}}. \tag{11}$$

2.3.2 Simplified model for the retort dynamics

The solution of Eqs. (5)-(11) involves the computation of the steam condensation flux (χ) at each integration step through Eq. (8). Because of the non-linearity of the equations involved, the solution of Eq. (8) must be obtained through an iterative procedure which hampers the simulation of the model. This is particularly relevant when the model is used for real-time tasks. To reduce the computational effort, a simplified version of the sterilization unit model was derived in Alonso et al. (1997). In this version, retort temperature evolution is described by:

$$\left[\frac{m_R c_{p,R}}{\lambda} - \left(\frac{BT_R}{(T_R - C)^2} + 1\right)\frac{V_v P_{eq}}{RT_R^2}\right]\frac{\mathrm{d}T_R}{\mathrm{d}t} = F_s^i - F_b - \frac{Q_l}{\lambda}. \tag{12}$$

Note that Eqs. (5)-(7) are not required in the simplified version. However, Eq. (12) cannot be used for describing the cooling stage. Therefore it will only be used during venting and holding stages, whereas Eqs. (6)-(9) will be used during the cooling stage.

The retort temperature is regulated by a PI controller acting on the steam valve:

$$u_{s,k} = u_{s,k-1} + K_p\left(1.0 + \frac{\Delta t}{\tau_I}\right)\epsilon_k - K_p \epsilon_{k-1}, \tag{13}$$

where ϵ_k is the difference between the retort temperature and the reference trajectory at time t_k, i.e $\epsilon_k = T_{R,sp}(t_k) - T_R(t_k)$. $u_{s,k}$ represents the steam valve opening in during the time interval $t \in [t_k, t_{k+1}]$.

2.4 Safety and quality indicators

Microbial lethality (F_0), which is typically used as the safety indicator, is described by:

$$\frac{\mathrm{d}F_0}{\mathrm{d}t} = 10^{\frac{T_c(t)-T_{ref}}{z_{F,ref}}}, \tag{14}$$

where $T_c(t)$ is the temperature at the coldest point (the center) of the food product. In this work, $F_0 \geq 8$ min will be used as the lethality value to be reached at the end of the process, although other (less conservative) values could be considered as well.

Heating has a negative effect on food quality either defined as nutrient or organoleptic indicators (e.g. color or texture). Surface color (C_s) has been extensively used as a quality indicator for canned tuna both in the literature (Banga et al., 1993; Scherer et al., 2009; Sendin et al., 2010; Mohan et al., 2014; Rueangwatcharin and Wichienchot, 2015) and in canneries. Typically, when canneries produce *gourmet* articles (highly appreciated by consumers), they use less aggressive sterilization strategies that result into whiter tuna, at the price of reducing productivity. Therefore, in this work, surface color is used as the quality indicator. Degradation of C_s can be described using a Thermal Death Time (TDT) kinetics of the form (Banga et al., 1993):

$$\frac{\mathrm{d}\log_{10} C_s}{\mathrm{d}t} = -\frac{1}{D_{ref}} 10^{\frac{T_s(t)-T_{ref}}{z_{C,ref}}}. \tag{15}$$

where $T_s(t)$ is the temperature on the top surface of the solid food product.

2.5 Multi-objective optimization under product variability

In this section, we will formulate the optimization problem with multiple objectives (such as process time, average food product quality, and uniformity) when variability on the food product is considered. Variability in the thermal coefficients (α_p, h_t and h_b) affects both safety and quality indicators. The operation strategy of the sterilization process must be such that all items in the batch fulfill the requirement of safety (lethality). Regarding the quality indicator (surface color), variability might cause that thermal treatments with good average quality contain some items with much poorer quality. Uniformity is, therefore, an important issue to be considered together with the average quality. Process time is also a relevant objective to increase plant productivity. Other objectives, such as other quality indicators (nutrient degradation, texture, etc.) or process energy consumption could be also considered. However, for the sake of clarity in the presentation, in this work we will only consider:

- To maximize the average color retention (μ_{C_s}).
- To minimize surface color variability (σ_{C_s}), i.e maximize uniformity.
- To minimize batch sterilization time (t_f).

This constitutes a multi-objective dynamic optimization problem (MODOP) with many potential optimal solutions depending on the preferred trade off among objectives (Miettinen, 1998). The decision variable in this problem is the reference trajectory of the retort temperature ($T_{R,sp}(t)$). Mathematically, the MODOP can be written as:

$$\min_{T_{R,sp}(t)} J := [-\mu_{C_s}, \sigma_{C_s}, t_f] \in \mathbb{R}^3. \tag{16}$$

Subject to:

- The food product dynamics, Eq. (4).
- The retort dynamics, including the PI controller, Eqs. (5)-(13).
- Safety and quality indicators dynamics, Eqs. (14) and (15), respectively.
- Final lethality of the food product in all items of the batch, $F_0(t_f) \geq 8.0$ min.
- Final temperature at the central point of all food items, $T_c(t_f) \leq 90$ °C.

The last temperature constraint is to ensure that the product does not continue to degrade once the batch is finished. Besides, since canneries usually work with retort temperatures in a given interval, we will also consider the following bounds on the decision variable $105°\text{C} \leq T_{R,sp}(t) \leq 130°\text{C}$. Note, however, that different bounds could be taken into account.

Usual approaches aiming at maximizing average quality or uniformity are based on Monte-Carlo simulations that allow the computation of μ_{C_s} and σ_{C_s} (Baucour et al., 2003; Smout et al., 2003). However, this is not practical for real-time implementations as thousands of simulations have to be performed at each step of the optimization procedure. This is particularly relevant when variability in more than one parameter is considered. In the remaining of this section, we will show that optimization of both average color retention and color variability is possible without the need of performing thousands of simulations covering the whole uncertain-parameter space.

Let us recall the mean and standard deviation values for the thermal parameters α_p, h_t and h_b presented in Section 2.2. Then, according to this variability characterization, the following region of parameter uncertainty can be defined:

$$\begin{aligned}\Omega := \Big\{\alpha_p, h_t, h_b \,|\, & \mu_{\alpha_p} - c\sigma_{\alpha_p} \leq \alpha_p \leq \mu_{\alpha_p} + c\sigma_{\alpha_p}, \\ & \mu_{h_t} - c\sigma_{h_t} \leq h_t \leq \mu_{h_t} + c\sigma_{h_t}, \\ & \mu_{h_b} - c\sigma_{h_b} \leq h_b \leq \mu_{h_b} + c\sigma_{h_b}\Big\}.\end{aligned} \tag{17}$$

In this work, we will follow the work by Baucour et al. (2003) and use $c = 3$, for which the region Ω includes 99.7% of the parameter values in the Gaussian distribution. Note that Ω is a polytopic convex set defined by 2^3 vertices.

Besides, note that heat transfer is slower in those items with lower values of the thermal parameters. Therefore, quality degradation will be also slower in these items (monotonic response of the safety and quality indicators with respect to the thermal parameters). Hence, the maximum (minimum) quality will be reached in the items with the lowest (largest) values of the thermal parameters. Let us denote by $C_{s,max}$ and $C_{s,min}$ the final surface color obtained with the minimum and maximum values of the parameters:

$$C_{s,max} := C_s(t_f, \mu_{\alpha_p} - 3\sigma_{\alpha_p}, \mu_{h_t} - 3\sigma_{h_t}, \mu_{h_b} - 3\sigma_{h_b}),$$

$$C_{s,min} := C_s(t_f, \mu_{\alpha_p} + 3\sigma_{\alpha_p}, \mu_{h_t} + 3\sigma_{h_t}, \mu_{h_b} + 3\sigma_{h_b}).$$

In this way, we can use $(C_{s,max} - C_{s,min})$ to fully characterize quality variability (up to the confidence level $c = 3$) instead of computing σ_{C_s} from thousands of simulations in a Monte-Carlo scheme.

Analogously, the lowest final lethality value will correspond to the item with the slowest heat flow, i.e. with the lowest values of the thermal coefficients:

$$F_{0,min} = F_0(t_f, \mu_{\alpha_p} - 3\sigma_{\alpha_p}, \mu_{h_t} - 3\sigma_{h_t}, \mu_{h_b} - 3\sigma_{h_b}).$$

The monotonic property with respect to the thermal parameters can also be exploited to (conservatively) ensure $T_c(t_f) \leq 90$ °C for all food items. Note that, given the proposed retort-temperature bounds, $T_c(t_h) \leq 130$ °C for all items at the end of the holding stage (thermal equilibrium would set $T_R = T_s = T_c = 130$). Therefore, assuming the worst case, i.e. the central point of the food item with slower heat transfer reached the highest possible temperature, we propose to set the duration of the cooling stage (t_c) by solving a boundary value problem (BVP) with the food-product dynamics (4), retort cooling dynamics (5)-(11), and the following boundary conditions:

$$\begin{aligned} &T_R(0) = 130\ ^\circ\text{C}, \\ &T_c(0, \mu_{\alpha_p} - 3\sigma_{\alpha_p}, \mu_{h_t} - 3\sigma_{h_t}, \mu_{h_b} - 3\sigma_{h_b}) = 130\ ^\circ\text{C}, \\ &T_c(t_c, \mu_{\alpha_p} - 3\sigma_{\alpha_p}, \mu_{h_t} - 3\sigma_{h_t}, \mu_{h_b} - 3\sigma_{h_b}) = 90\ ^\circ\text{C}. \end{aligned} \tag{18}$$

Consequently, the total batch time will be the time of the holding stage (variable) plus the one of the cooling stage (fixed in advance by the above BVP): $t_f = t_h + t_c$.

Finally, Jensen's inequality (Perlman, 1974) states that: *for a random variable x taking values in the domain of a convex function f, the mathematical expectation* (E) *of $f(x)$ is larger than (or equal to) f applied to the mathematical expectation of x*, i.e. $\mathrm{E}(f(x)) \geq f(\mathrm{E}(x))$. Therefore, instead of computing the mean value of color μ_{C_s} from thousands of simulations in a Monte-Carlo scheme, we can set a lower bound for the average surface color using the mean value of the thermal parameters, i.e:

$$\bar{C}_s := C_s(t_f, \mu_{\alpha_p}, \mu_{h_t}, \mu_{h_b}).$$

Hence, problem (16) is recast to solving:

$$\min_{T_{R,sp}(t)} J := [-\bar{C}_s, C_{s,max} - C_{s,min}, t_f] \in \mathbb{R}^3. \tag{19}$$

Subject to:

- The food product dynamics, Eq. (4).
- The retort dynamics, including the PI controller, Eqs. (5)-(13).
- Safety and quality indicators dynamics, Eqs (14) and (15), respectively.
- Minimum final lethality, $F_{0,min} \geq 8.0$ min.
- Bounds on the reference trajectory, $105°C \leq T_{R,sp}(t) \leq 130°C$

Note that solving the MODOP (19) involves performing only three simulations of the model at each optimization step: One to compute $C_{s,min}$ (using the maximum value of the thermal parameters), another one to compute $\bar{C}_s$ (using the mean value of the thermal parameters), and another one to compute $C_{s,max}$ and $F_{0,min}$ (using the minimum value of the thermal parameters).

The control vector parameterization (CVP) approach is selected, among the different options (Biegler et al., 2002; Vilas et al., 2012), to describe the reference trajectory ($T_{R,sp}(t)$). The CVP proceeds dividing the process duration into a number of elements and approximating $T_{R,sp}(t)$, typically using low order polynomials which become the new decision variables. In this work, we divided the venting and holding stages duration into a number (n) of intervals equally spaced[1]. The decision variables for optimization are, therefore, the reference trajectory temperature values at the boundaries of such intervals ($T_{R,sp}(t_k)$, with $k = 1, 2, \ldots, n+1$) and the duration of the holding stage (t_h). The CVP approach allows us, then, to re-write the infinite-programming MODOP (19) as:

$$\min_{T_{R,sp}(t_k), t_h \in \mathbb{R}^{n+2}} \quad J := [-\bar{C}_s, C_{s,max} - C_{s,min}, t_f] \in \mathbb{R}^3, \tag{20}$$

subject to constraints analogous to the ones in problem (19) above.

2.6 Online safety sensing and dynamic optimization under product variability

The scheme for event-based optimization proposed in this work is presented in Figure 2. First, a given reference trajectory for sterilizer temperature ($T_{R,sp}(t)$) is selected from the Pareto front obtained off-line by solving Problem (20). The PI controller uses this $T_{R,sp}(t)$ and the measured values in the retort ($T_R(t)$) to compute, according to Eq. (13), the steam valve openings (u_s).

[1]Intervals of different duration could be also considered. However, this may imply increasing the number of decision variables *ad hoc*.

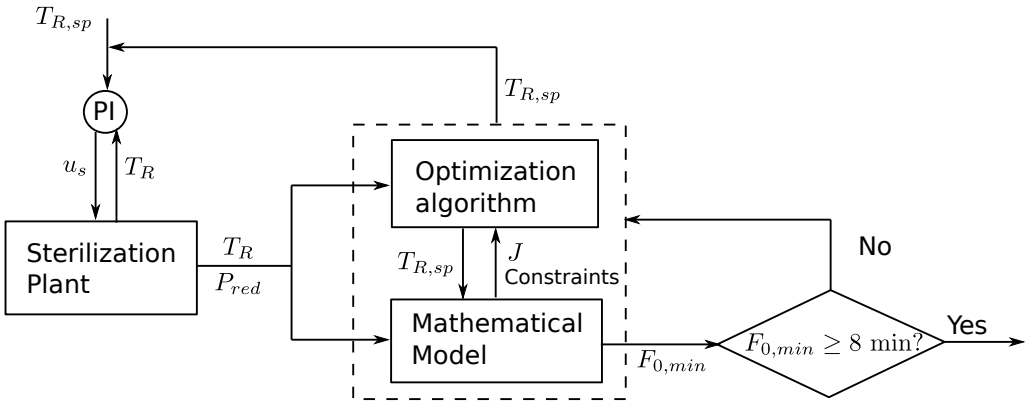

Figure 2: Illustrative scheme of the on-line safety sensing and event-based dynamic optimization approach.

Once the sterilization has started, available plant measurements (T_R and P_{red}) are fed to the mathematical model. The model acts as as a *software sensor*, using these measurements to predict, in real-time, the microbial lethality that the item with the slower heat transfer will reach at the end of the sterilization ($F_{0,min}$). If the safety requirement is fulfilled ($F_{0,min} \geq 8$ min), the process continues with no action on the original reference trajectory. On the contrary, if plant perturbations arise such that the predicted $F_{0,min} < 8$ min, then the optimization scheme computes a corrective reference trajectory[2] from the current plant state, that is passed to the PI controller. Obviously, in this contingency situation, the optimization problem must be solved on-line. Therefore, computing and analyzing all Pareto optimal solutions by (20) is not practical due to the demanding time constraints. For this reason, the different objectives in the MODOP are weighted in a linear combination according to the plant-engineers preferences. In this way, the MODOP becomes a single-objective dynamic optimization problem (SODOP):

$$\min_{T_{R,sp}(t_k),t_h \in \mathbb{R}^{n+2}} J = -w_1 \frac{\bar{C}_s}{C_s^*} + w_2 \frac{C_{s,max} - C_{s,min}}{\Delta C_s^*} + w_3 \frac{t_f}{t_f^*}, \tag{21}$$

subject to the same constraints presented in the previous section. Although this option is quite common in practice, it must be pointed out that the performance of the obtained solution highly depends on the chosen weights (w_1, w_2, w_3). Besides, other hidden solutions in the Pareto front, that cannot be revealed by this approach, may exist (Reynoso-Meza, 2014). Parameters C_s^*, ΔC_s^* and t_f^* in Eq. (21) are used to normalize individual objectives so that they are in the same order of magnitude.

The MEIGO toolbox (Egea et al., 2014) is used to find the solution of the SODOP problems. This toolbox includes several metaheuristic methods among which, the enhanced scatter search metaheuristic (eSS) (Egea et al., 2010) is selected. This eSS solver combines the scatter search approach, to escape from local optima, and local optimization methods,

[2]Differences between the optimal profiles computed off-line and on-line are mainly caused by perturbations in the steam pressure coming from boilers.

to enhance convergence to the global solution. Of course, solving the optimization elapses some time (5 min maximum in this case study), during which the plant continues running with the previous reference trajectory. This small time delay is already contemplated in the formulation to avoid discrepancies between the predicted final lethality and quality with the reality.

3 Results and Discussion

3.1 Multi-objective optimization under product variability

As previously mentioned, multi-objective optimization problems have many potentially optimal solutions. The selection of one solution or another will depend on the preferences on the objectives. Before proceeding with the event-based dynamic optimization problem, let us analyze the different solutions of the MODOP (20) obtained off-line. To this purpose, several options are available (Boada et al., 2016), among which we have chosen to proceed as follows. We first define a *pertinency region* (Reynoso-Meza, 2014). Outside this region the objectives are either not reachable or they degrade too much in terms of production efficiency or quality. Therefore, solutions outside the pertinency region are not considered. For instance, using the constraint $F_0(t_f) \geq 8$ min, and considering that the maximum temperature allowed in the retort is 130 °C, sterilizing faster than 40 min is not possible with this equipment. Besides, using operation strategies with duration larger than 130 min for RO200 containers would significantly reduce the productivity of the plant and, as it will be shown in this section, no relevant improvement in quality is achieved. Also, values of 40% in average color retention or 18% in the difference between the items with maximum and minimum color are considered of very poor quality and canneries do not work close to these limits. The limits set for the pertinency region in this work are, therefore:

$$\bar{C}_s \in [40, 75]\ \%, \quad (C_{s,max} - C_{s,min}) \in [0, 18]\ \%, \quad t_f \in [40, 130]\ \text{min}.$$

In this regard, note that upper bounds for $\bar{C}_s$ above 75% could be included. In this work, they have been neglected because, using this equipment and for this product, the established constraint $F_{0,min} \geq 8$ min prevents reaching higher values. Note, also, that these bounds could be included as constraints in the optimization problem (21). In this way, convergence to a point inside the pertinency region is ensured despite the selection of the weights. Now, we discretize the intervals of two of the objectives in a fixed number of points. For illustrative purposes, we have chosen to discretize $\bar{C}_s$ and $(C_{s,max} - C_{s,min})$ in $n_{\bar{C}_s} = n_{(C_{s,max}-C_{s,min})} = 20$ points. This defines a 2D grid with 400 intersection points.

Now, the MODOP is cast as a set of SODOP. To that purpose, we choose a given pair of $\bar{C}_s$ and $(C_{s,max} - C_{s,min})$ in the grid. These values are introduced as upper-bounded inequality constraints and the SODOP consists of finding the sterilization strategy that

minimizes t_f. This is repeated for the other 399 points in the grid to approximate the Pareto front.

Following the CVP strategy, the continuous reference trajectory ($T_{R,sp}$) is constrained to n piece-wise linear polynomials. In this case, we have chosen $n = 5$, what results in 7 decision variables, namely the temperature values at six time instants (t_k) as well as the duration of the holding (t_h) stage.

The Pareto front obtained from solving the 400 SODOPs is depicted in Figure 3. Since

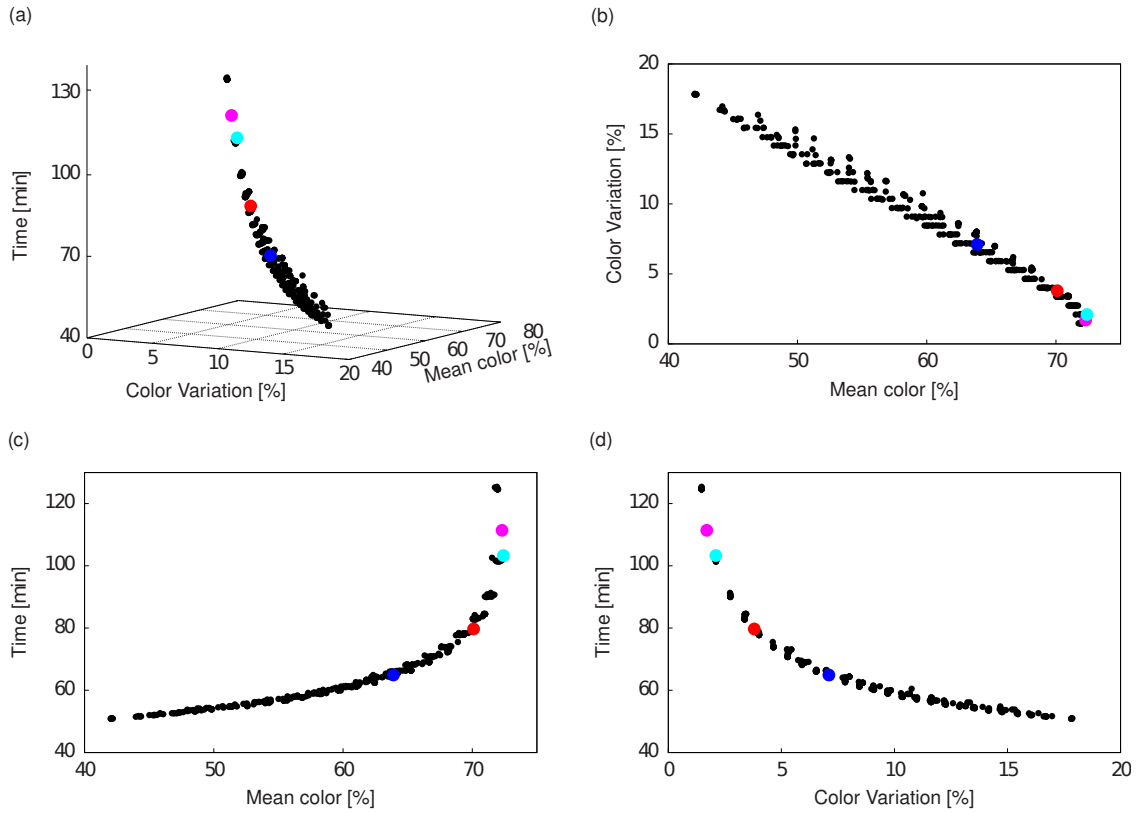

Figure 3: Pareto front obtained by solving the MODOP (20). (a) 3D representation, (b)-(d) 2D projections. Colored dots highlight some representative solutions.

the solutions obtained may be difficult to visualize and analyze in the 3D representation (Figure 3(a)), the different 2D projections are also included (Figure 3(b)-(d)). As shown in the figure, strategies with fast sterilization times result in high degradation of average surface color and uniformity. Note also that little quality improvement is obtained at strategies with processing times larger than 100 min. When the workload in the sterilizers of the plant is relatively low, the operator can select reference trajectories with processing times close to 100 min to improve quality and uniformity. On the contrary, if many carts containing the packed product are waiting for sterilization, faster strategies can be chosen to increase productivity and to avoid bottlenecks, at the price of getting lower product quality and/or uniformity of course.

For illustrative purposes, Figure 3 also highlights four qualitatively different solutions

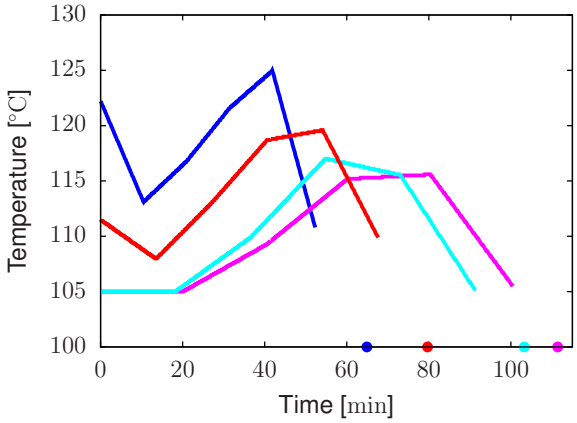

Figure 4: Optimal reference trajectories for the retort temperature obtained by solving Problem (21) using different weights for the individual objectives. Dots in the x-axis just indicate the end time of the cooling stage.

that can be obtained by solving Problem (21) with different weights in the individual objectives. The values used to normalize the individual objectives are chosen as the upper bounds of the pertinency region, i.e. $C_s^* = 75\%$, $\Delta C_s^* = 18\%$ and $t_f^* = 130$ min. The blue point in Figure 3 was obtained by giving more importance to process time ($w_1 = 1$, $w_2 = 5$ and $w_3 = 20$), whereas the solutions marked as cyan ($w_1 = 20$, $w_2 = 1$ and $w_3 = 1$) and magenta ($w_1 = 5$, $w_2 = 20$ and $w_3 = 5$) prioritize average quality and quality variability, respectively. Finally, the red point corresponds with an intermediate solution ($w_1 = 4$, $w_2 = 1$ and $w_3 = 3$). The profiles obtained for each of these cases are depicted in Figure 4 whereas the optimal values of each individual objectives for the blue, cyan, magenta and red points are shown in Table 2. As mentioned before, process time, average quality and uniformity largely depend on the selected weights. As expected, more aggressive strategies with higher retort temperatures result into shorter processing times whereas using smoother temperatures benefit product quality.

Table 2: Values obtained for the individual objectives using different weights in Problem (21).

Point	$C_s(t_f)$ [%]	$\left(C_{s,max}(t_f) - C_{s,min}(t_f)\right)$ [%]	t_f [min]
Blue	63.9	7.1	64.9
Cyan	72.4	2.1	103.3
Magenta	72.3	1.7	111.4
Red	70.1	3.8	79.7

The sterilization strategy for the solution marked as a red dot is represented in Figure 5. Subplot 5(a) shows the evolution of the temperature in the sterilizer (gray line); at the product surface (blue band); and at the center of the food product (red band). Limits of the bands are defined by the simulation results obtained with the minimum and maximum values of the thermal parameters, within the variability region Ω defined in Eq. (17). The dashed line represents the reference trajectory of the sterilizer obtained as the solution

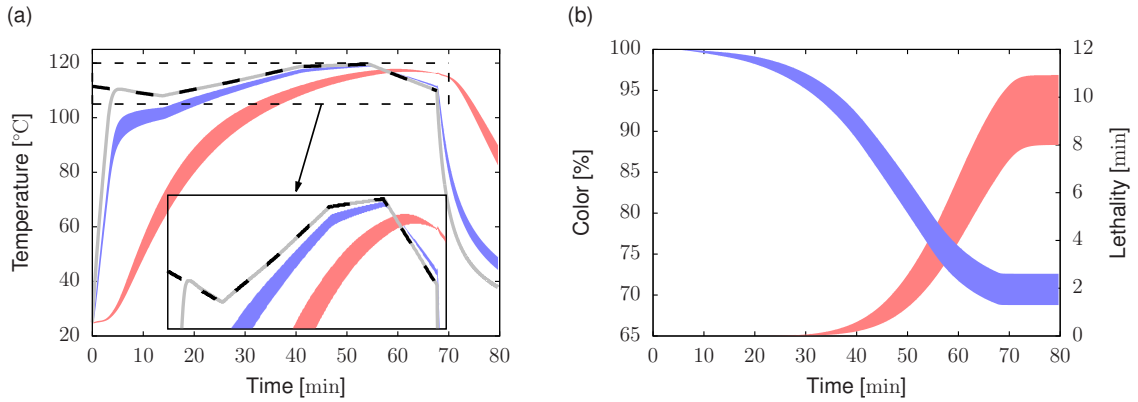

Figure 5: Sterilization strategy obtained using the approach of weighting the objectives to obtain a SODOP. Weights used are $w_1 = 4$, $w_2 = 1$ and $w_3 = 3$. The subplots show the evolution of (a) Retort and product temperatures, (b) lethality (red) and surface color (blue).

of problem (21). Note that, at the end of the process, the temperature at the center of the food product for all items is lower than 90 °C, as desired. Subplot 5(b) shows the evolution of the microbial lethality for the different items in a batch. As in Subplot 5(a), the limits of the bands correspond with the simulations performed using the minimum and maximum values of the thermal parameters. The minimum value of F_0 at the end of the process, i.e. $F_{0,min}$, is larger than (although close to) 8 min, which means that all items in the batch fulfill the required safety constraint. Evolution of surface-color retention is also included in Subplot 5(b). It can be seen that average color retention is close to 70% and the difference between the maximum and minimum values is lower than 4%. Consequently, implementing this sterilization strategy is expected to provide products with good average quality (close to the maximum possible) and uniformity.

3.2 On-line safety sensing and event-based dynamic optimization under product variability

In canneries, resources such as steam may be shared by several sterilization units or other equipment, such as can-washing machines or cookers. Thus, when several units, whose correct operation depends on shared resources, are working at the same time, pressure drops might occur if resource generation (e.g. boilers) is not capable of fulfilling the demand at nominal conditions. Besides, faults in the boiler might occur during the sterilization procedure. These disturbances prevent the perfect tracking of the reference temperature trajectory. In these cases, the lethality constraint might not be fulfilled for some or all the items of the batch, with the corresponding rejection or reprocessing of the whole batch.

To illustrate this point, let us consider the optimal sterilization strategy obtained by solving the SODOP (21) with $w_1 = 4$, $w_2 = 1$ and $w_3 = 3$ (Figure 5). At $t = 28.2$ min we simulate a fault in the boiler that makes the input steam pressure (P_{red}) to drop from

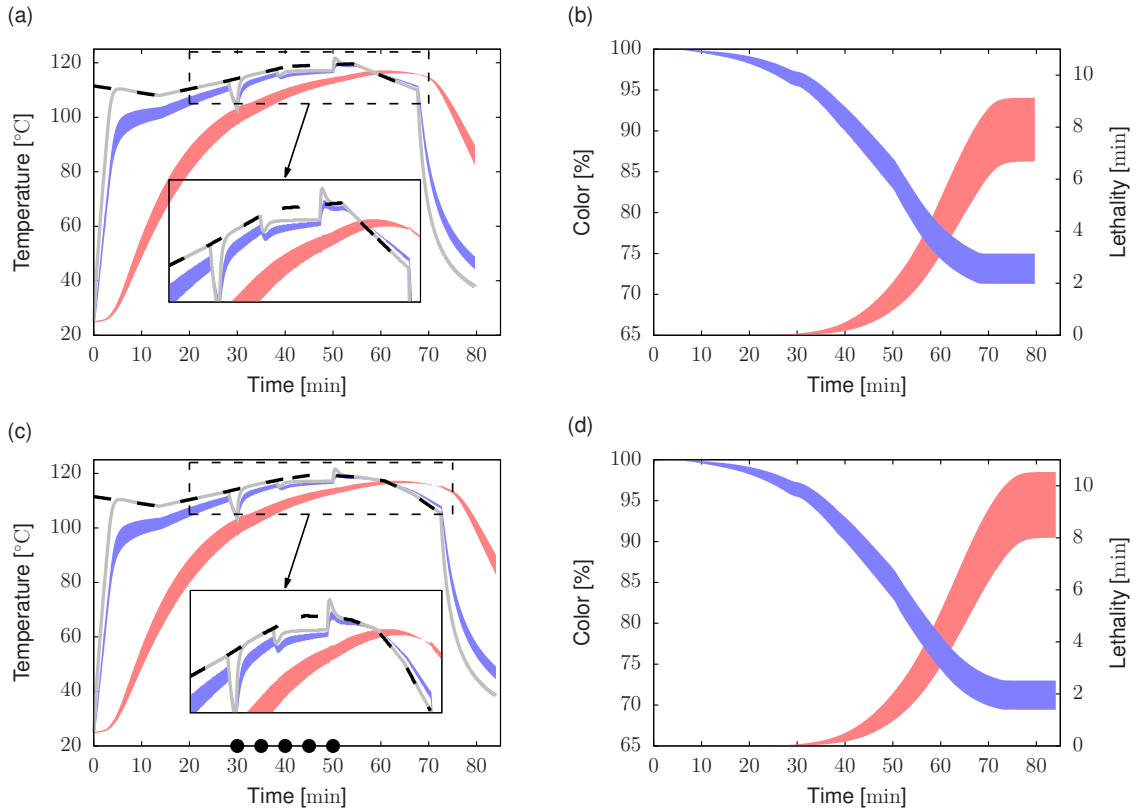

Figure 6: Top figures: effect of a perturbation in the input steam pressure on the sterilization strategy obtained from the Pareto front. Bottom figures: on-line update of the sterilization profile after the perturbation occurs. The subplots (a) and (c) show the evolution of retort and product temperatures, whereas (b) and (d) show the lethality (red) and surface color (blue) respectively. Black dots in subplot (c) indicate the times at which the reference trajectory is updated.

3.54×10^5 Pa to 0 Pa. After 1.7 min the boiler recovers. Then, at time $t = 38.2$ min, we simulate the effect of having several retorts, that use the same steam source, working at the same time. In this case, P_{red} drops from 3.54×10^5 Pa to 2.03×10^5 Pa. As shown in Figure 6(a), when the perturbations are introduced, the retort is not able to track the reference trajectory. This has an important effect on the lethality reached by the items in the batch (Figure 6(b)). Note that, although the highest final lethality is above 8 min, many items in the batch are clearly below this safe value, as $F_{0,min}$ is 6.7 min.

As shown in the bottom subplots of Figure 6, the batch can be saved if the final microbial lethality is predicted by the model using available plant measurements. When a process perturbation is large enough to prevent all items from reaching the safety constraint, a new sterilization profile is recomputed by the optimization routine following the methodology proposed in Section 2.6. This is, the event-based optimization triggers when the software sensor predicts that the safety constraint will not be reached at the end of the batch (disturbances that cannot be compensated quickly by the PI control loop is detected). Then, a corrective strategy for finishing the sterilization is computed by the

SODOP (21). In this case, the reference trajectory is recomputed five times during the batch (black dots in Figure 6(c)). The remaining $T_{R,sp}(t_k)$ (i.e. those not yet implemented at current time) as well as a new heating time t_h are the decision variables in the SODOP. Note that solving the SODOP to full optimality can elapse a several minutes with the employed setup. In this case study, 5 min of computation is considered an acceptable limit to stop the optimization obtaining reasonably optimal solutions. During this time-lapse, the plant continues running with the previous reference trajectory. Our event-based approach takes this issue into account by using the model to predict the evolution of the plant during these 5 minutes with the previous control reference.

The updated reference trajectory is presented in Figure 6(c) together with its effect on the retort temperature (gray line), as well as the temperature at the product surface (red bands) and product center (blue bands). As shown in Figure 6(d), the new sterilization strategy results into a batch with $F_{0,min} \geq 8$ min. Besides, since the new strategy was optimally computed, process duration is only increased by 4 min with respect to the original strategy and the effect on quality degradation is minimal (Figure 6(d)).

The reader may realize that, although the final safety constraints are fulfilled, part of the recomputed optimal trajectory is also above the heating capacities of the retort. This is because all sterilization profiles above such capacities result in the same value of the objective function (zero sensitivity of the model outputs with respect to decision variables) so the optimization algorithm cannot distinguish among them. Nevertheless, this does not create any problem, as happened with the initial reference after the disturbance, because final lethality is well predicted by the model in current process conditions. Anyway, an additional term that penalizes solutions above unreachable temperatures could be added to the cost function to overcome this little inconvenience.

4 Conclusions

In this contribution, we presented a closed-loop control framework that uses model-based optimization to deal with unexpected disturbances in sterilization processes. It is well known that such disturbances might compromise the requirements of food safety, even more with the variability inherent to the food products, leading to the rejection of the batch in the worst case. To avoid this issue, we have derived and implemented a software sensor together with an event-based strategy that make use of available plant measurements to recompute the thermal processing profile when unexpected perturbations occur. The approach takes into account variability among the food items to be processed and multiple objectives simultaneously in a mathematical optimization fashion. For illustrative purposes, the objectives considered were the minimization of the process duration as well as the maximization of average surface color retention and uniformity among the items in the batch. Other objectives such as energy consumption or other quality indicators can be easily included in the methodology. Monotonicity and convexity properties of

the safety/quality indicators were used to efficiently evaluate food safety, average quality, and uniformity. We showed that the profiles recomputed using our methodology allow to guarantee that, even under the presence of plant disturbances, food safety requirements are met, while minimizing, at the same time, their influence on food quality, uniformity, and process duration.

Once the safety sentinel is deployed, the replacement of the limited PI control loops by a real-time optimal control, a.k.a. economic model-predictive control, might be the next evident step. However, the times to solve the SODOP need to be reduced drastically in this case. A way to achieve this could be coding the SODOP in a software environment that provides exact sensitivities and algorithmic differentiation (Andersson et al., 2019), so that gradient-based solvers can run efficiently. Besides, the use of computing strategies that allow to run in parallel the three required simulations (i.e. using the minimum, mean and maximum values of the thermal parameters) will be studied too. Finally, we would like to integrate this approach into the recently developed scheduling algorithms with redundant equipment and shared resources (Palacin and de Prada, 2019). The benefits would be twofold: The off-line MODOP provides a static database of thermal treatments among which the scheduling tool can choose, depending on the factory situation; whilst the on-line routine guarantees product safety and can give feedback of actual operation to the scheduler.

Acknowledgments

Authors C. Vilas, L. Taboada, and J.L. Pitarch would like to dedicate this contribution to Prof. Antonio A. Alonso, the researcher that inspired this work, which unfortunately passed away. We thank his endless support and continuous guidance.

This research received funding by the Spanish MICINN with FEDER funds (PGC2018-099312-B-C31, PGC2018-099312-B-C33).

References

A. Abakarov, Y. Sushkov, S. Almonacid, and R. Simpson. Multiobjective optimization approach: thermal food processing. *Journal of Food Science*, 74(9):E471–E487, 2009. doi: https://doi.org/10.1111/j.1750-3841.2009.01348.x.

A. A. Alonso, J. R. Banga, and R. I. Pérez-Martín. A complete dynamic model for the thermal processing of bioproducts in batch units and its application to controller design. *Chemical Engineering Science*, 52(8):1307–1322, 1997. doi: https://doi.org/10.1016/S0009-2509(96)00484-8.

A. A. Alonso, A. Arias-Méndez, E. Balsa-Canto, M. R. García, J. I. Molina, C. Vilas, and M. Villafín. Real time optimization for quality control of batch thermal sterilization

of prepackaged foods. *Food Control*, 32(2):392–403, 2013. doi: https://doi.org/10.1016/j.foodcont.2013.01.002.

J. A. E. Andersson, J. Gillis, G. Horn, J. B. Rawlings, and M. Diehl. CasADi – A software framework for nonlinear optimization and optimal control. *Mathematical Programming Computation*, 11(1):1–36, 2019. doi: 10.1007/s12532-018-0139-4.

M. R. Ansorena and V. O. Salvadori. Optimization of thermal processing of canned mussels. *Food Science and Technology International*, 17(5):449–458, 2011. doi: https://doi.org/10.1177/1082013211398829.

E. Ávila-Gaxiola, F. Delgado-Vargas, J. Zazueta-Niebla, G. López-Angulo, M. Vega-García, and J. Caro-Corrales. Variable retort temperature profiles for canned papaya puree. *Journal of Food Process Engineering*, 39:11–18, 2016. doi: https://doi.org/10.1111/jfpe.12194.

E. Balsa-Canto, J. R. Banga, and A. A. Alonso. A novel, efficient and reliable method for thermal process design and optimization. part II: Applications. *Journal of Food Engineering*, 52(3):235–247, 2002. doi: https://doi.org/10.1016/S0260-8774(01)00111-X.

J. R. Banga, A. A. Alonso, J. M. Gallardo, and R. I. Pérez-Martín. Kinetics of thermal degradation of thiamine and surface colour in canned tuna. *Zeitschrift fur Lebensmittel-Untersuchung und Forschung*, 197(2):137–131, 1993. doi: https://doi.org/10.1007/BF01260307.

J. R. Banga, Z. Pan, and R. P. Singh. On the optimal control of contact-cooking processes. *Food and Bioproducts Processing*, 79(C3):145–151, 2001. doi: https://doi.org/10.1205/096030801750425235.

J. R. Banga, E. Balsa-Canto, and A. A. Alonso. Quality and safety models and optimization as part of computer-integrated manufacturing. *Comprehensive Reviews in Food Science and Food Safety*, 7(1):168–174, 2008. doi: https://doi.org/10.1111/j.1541-4337.2007.00023.x.

P. Baucour, K. Cronin, and M. Stynes. Process optimization strategies to diminish variability in the quality of discrete packaged foods during thermal processing. *Journal of Food Engineering*, 60:147–155, 2003. doi: https://doi.org/10.1016/S0260-8774(03)00028-1.

L. Biegler, A. Cervantes, and A. Wätcher. Advances in simulaneous strategies for dynamic process optimization. *Chemical Engineering Science*, 57(4):575–593, 2002. doi: https://doi.org/10.1016/S0009-2509(01)00376-1.

Y. Boada, J. L. Pitarch, A. Vignoni, G. Reynoso-Meza, and J. Picó. Optimization alternatives for robust model-based design of synthetic biological circuits. *IFAC-PapersOnLine*, 49(7):821–826, 2016. doi: https://doi.org/10.1016/j.ifacol.2016.07.291.

A. S. Chalabi, L. G. van Willigenburg, and G. van Straten. Robust optimal receding horizon control of the thermal sterilization of canned foods. *Journal of Food Engineering*, 40(3):207–218, 1999. doi: https://doi.org/10.1016/S0260-8774(99)00057-6.

C. R. Chen and H. S. Ramaswamy. Multiple ramp-variable retort temperature control for optimal thermal processing. *Food and Bioproducts Processing*, 82(C1):78–88, 2004. doi: https://doi.org/10.1205/096030804322985353.

K. Cronin, K. Abodayeh, J. Caro-Corrales, A. Pokrovskii, and A. Demir. Probabilistic studies of the thermal processing of discrete solid products. *Food and Bioproducts Processing*, 78(C):126–132, 2000. doi: https://doi.org/10.1205/096030800532860.

K. Cronin, D. Mackey, V. Cregan, S. O'Brien, J. P. Gleeson, and K. Abodayeh. Selection of processing temperature to minimize product temperature variability in food heating processes. *Food and Bioproducts Processing*, 85(4):344–353, 2007. doi: https://doi.org/10.1205/fbp07080.

A. D. Demir, P. Baucour, D. Cronin, and K. Abodayeh. Analysis of temperature variability during the thermal processing of hazelnuts. *Innovative Food Science and Emerging Technologies*, 4(1):69–84, 2003. doi: https://doi.org/10.1016/S1466-8564(02)00084-X.

J. A. Egea, R. Martí, and J. R. Banga. An evolutionary method for complex-process optimization. *Computers and Operations Research*, 37(2):315–324, 2010. doi: https://doi.org/10.1016/j.cor.2009.05.003.

J. A. Egea, D. Henriques, T. Cokelaer, A. F. Villaverde, A. MacNamara, D. P. Danciu, J. R. Banga, and J. Saez-Rodriguez. Meigo: an open-source software suite based on metaheuristics for global optimization in systems biology and bioinformatics. *BMC Bioinformatics*, 15(136), 2014. doi: https://doi.org/10.1186/1471-2105-15-136.

F. Erdogdu and M. O. Balaban. Complex method for nonlinear constrained multi-criteria (multi-objective function) optimization of thermal processing. *Journal of Food Process Engineering*, 26(4):357–375, 2003. doi: https://doi.org/10.1111/j.1745-4530.2003.tb00607.x.

J. Flores-Cerrillo and J. F. MacGregor. Latent variable MPC for trajectory tracking in batch processes. *Journal of Process Control*, 15(6):651–663, 2005. doi: https://doi.org/10.1016/j.jprocont.2005.01.004.

M.-S. G. García, E. Balsa-Canto, A. A. Alonso, and J. R. Banga. Computing optimal operating policies for the food industry. *Journal of Food Engineering*, 74(1):13–23, 2006. doi: https://doi.org/10.1016/j.jfoodeng.2005.02.011.

T. Kondakci and W. Zhou. Recent applications of advanced control techniques in food industry. *Food and Bioprocess Technology*, 10:522–542, 2017. doi: https://doi.org/10.1007/s11947-016-1831-x.

Z. Kurtanjek. Opportunities and challenges of model predictive control in food technologies. In *Proceeding of the 4th Central European Congress of Food, Biotechnologists and Nutritionists, Cavtat, Croatia*, pages 105–110, 2008.

A. R. Lespinard, R. R. Bambicha, and R. H. Mascheroni. Quality parameters assessment in kiwi jam during pasteurization. modelling and optimization of the thermal process. *Food and Bioproducts Processing*, 90(4):799–808, 2012. doi: https://doi.org/10.1016/j.fbp.2012.03.001.

S. A. H. Lim, J. Antony, and S. Albliwi. Statistical process control (SPC) in the food industry - a systematic review and future research agenda. *Trends in Food Science & Technology*, 37(2):137–151, 2014. doi: https://doi.org/10.1016/j.tifs.2014.03.010.

M. Madoumier, G. Trystram, P. Sébastian, and A. Collignan. Towards a holistic approach for multi-objective optimization of food processes: A critical review. *Trends in Food Science & Technology*, 86:1–15, 2019. doi: https://doi.org/10.1016/j.tifs.2019.02.002.

K. Miettinen. *Nonlinear Multiobjective Optimization*, volume 12 of *International Series in Operations Research & Management Science*. Springer, Boston, MA, 1998. ISBN 9781461555643. doi: https://doi.org/10.1007/978-1-4615-5563-6.

T. Miri, A. Tsoukalas, S. Bakalis, E. N. Pistikopoulos, B. Rustem, and P. J. Fryer. Global optimization of process conditions in batch thermal sterilization of food. *Journal of Food Engineering*, 87:485–494, 2008. doi: https://doi.org/10.1016/j.jfoodeng.2007.12.032.

C. O. Mohan, S. Remya, C. N. Ravishankar, P. K. Vijayan, and T. K. S. Gopal. Effect of filling ingredient on the quality of canned yellowfin tuna (thunnus albacares). *International Journal of Food Science and Technology*, 49:1557–1564, 2014. doi: https://doi.org/10.1111/ijfs.12452.

S. Mortimore and C. Wallace. *HACCP: A practical approach*. Springer Science & Business Media, 2013.

B. M. Nicolaï, P. Verboven, N. Scheerlinck, and J. De Baerdemaeker. Numerical analysis of the propagation of random parameter fluctuations in time and space during thermal food processes. *Journal of Food Engineering*, 38(3):259–278, 1998. doi: https://doi.org/10.1016/S0260-8774(98)00108-3.

B. M. Nicolaï, J. A. Egea, N. Scheerlinck, J. R. Banga, and A. K. Datta. Fuzzy finite element analysis of heat conduction problems with uncertain parameters. *Journal of Food Engineering*, 103:38–46, 2011. doi: https://doi.org/10.1016/j.jfoodeng.2010.09.017.

C. Palacin and C. de Prada. Optimal coordination of batch processes with shared resources. In *12th IFAC Symposium on Dynamics and Control of Process Systems, including Biosystems, (DYCOPS 2019), IFAC, Florianópolis, Brasil*, 2019.

R. Peesel, M. Philippa, G. Schumma, J. Hesselbacha, and T. Walmsleyb. Energy efficiency measures for batch retort sterilization in the food processing industry. *Chemical Engineering Transactions*, 52:163–168, 2016. doi: https://doi.org/10.3303/CET1652028.

M. D. Perlman. Jensen's inequality for a convex vector-valued function on an infinite-dimensional space. *Journal of Multivariate Analysis*, 4(1):52–65, 1974. doi: https://doi.org/10.1016/0047-259X(74)90005-0.

G. Reynoso-Meza. *Controller Tuning by Means of Evolutionary Multiobjective Optimization: a Holistic Multiobjective Optimization Design Procedure.* PhD thesis, Universitat Politècnica de Valencia, Spain, 2014. URL `http://hdl.handle.net/10251/38248`.

U. Rueangwatcharin and S. Wichienchot. Development of functional canned and pouched tuna products added inulin for commercial production. *Journal of Food Science and Technology*, 52:5093–5101, 2015. doi: https://doi.org/10.1007/s13197-014-1589-y.

E. Scherer, A. Sandoval, and J. A. Barreiro. Kinetics of heat-induced color change of a tuna-vegetable mixture. *Interciencia*, 34(12):888–892, 2009.

J. O. H. Sendin, A. A. Alonso, and J. R. Banga. Efficient and robust multi-objective optimization of food processing: A novel approach with application to thermal sterilization. *Journal of Food Engineering*, 98(3):317–324, 2010. doi: https://doi.org/10.1016/j.jfoodeng.2010.01.007.

R. Simpson, S. Almonacid, and M. Mitchell. Mathematical model development, experimental validation and process optimization: retortable pouches packed with seafood in cone frustum shape. *Journal of Food Engineering*, 63:153–162, 2004. doi: https://doi.org/10.1016/S0260-8774(03)00294-2.

R. Simpson, A. Abakarov, and A. Teixeira. Variable retort temperature optimization using adaptive random search techniques. *Food Control*, 19(11):1023–1032, 2008. doi: https://doi.org/10.1016/j.foodcont.2007.10.010.

R. Simpson, D. Jimenez, S. Almonacid, H. Nunez, M. Pinto, C. Ramirez, O. Vega-Castro, L. Fuentes, and A. Angulo. Assessment and outlook of variable retort temperature profiles for the thermal processing of packaged foods: Plant productivity, product quality, and energy consumption. *Journal of Food Engineering*, 275(109839):1–8, 2020. doi: https://doi.org/10.1016/j.jfoodeng.2019.109839.

L. Sirovich. Turbulence and the dynamics of coherent structures. Part I: Coherent structures. *Quaterly of Applied Mathematics*, 45(3):561–571, 1987. doi: https://doi.org/10.1090/S0033-569X-1987-0910462-6.

C. A. Smith and A. B. Corripio. *Principles and practice of automatic process control*. J. Wiley, New York, 2nd edition, 1997.

C. Smout, A. M. L. Van Loey, and M. Hendrickx. Non-uniformity of lethality in retort processes based on heat distribution and heat penetration data. *Journal of Food Engineering*, 45(2):103–110, 2000. doi: https://doi.org/10.1016/S0260-8774(00)00046-7.

C. Smout, N. E. Banadda, A. M. L. Van Loey, and M. E. G. Hendrickx. Nonuniformity in lethality and quality in thermal process optimization: A case study on color degradation of green peas. *Journal of Food Science*, 68(2):545–550, 2003. doi: https://doi.org/10.1111/j.1365-2621.2003.tb05709.x.

A. Vande Wouwer, P. Saucez, and C. Vilas. *Simulation of ODE/PDE Models with MATLAB, OCTAVE and SCILAB: Scientific and Engineering Applications*. Springer, New York, 1st edition, 2014.

S. Varga, J. C. Oliveira, C. Smout, and M. E. Hendrickx. Modelling temperature variability in batch retorts and its impact on lethality distribution. *Journal of Food Engineering*, 44 (3):163–174, 2000. doi: https://doi.org/10.1016/S0260-8774(00)00021-2.

C. Vilas, E. Balsa-Canto, M. S. G. García, J. R. Banga, and A. A. Alonso. Dynamic optimization of distributed biological systems using robust and efficient numerical techniques. *BMC Systems Biology*, 6:79, 2012. doi: https://doi.org/10.1186/1752-0509-6-79.

C. Vilas, A. Arias-Méndez, M. R. García, A. A. Alonso, and E. Balsa-Canto. Toward predictive food process models: A protocol for parameter estimation. *Critical Reviews in Food Science and Nutrition*, 58(3):436–449, 2018. doi: https://doi.org/10.1080/10408398.2016.1186591.

C. Vilas, A. A. Alonso, E. Balsa-Canto, E. Lopez-Quiroga, and I. C. Trelea. Model-Based Real Time Operation of the Freeze-Drying Process. *Processes*, 8(3):325, 2020. doi: https://doi.org/10.3390/pr8030325.

A The proper orthogonal decomposition

In this section, a brief description of the *proper orthogonal decomposition* (POD) (Sirovich, 1987) applied to the thermal processing of solid food is provided.

For the sake of clarity, let us rewrite the food product equations:

$$\frac{\partial T_p}{\partial t} = \alpha_p \left[\frac{\partial^2 T_p}{\partial z^2} + \frac{1}{r} \frac{\partial}{\partial r} \left(r \frac{\partial T_p}{\partial r} \right) \right], \tag{22}$$

$$\alpha_p \left.\frac{\partial T_p}{\partial z}\right|_{z=L} = h_t \left(T_R - T_p\big|_{z=L}\right),$$
$$\alpha_p \left.\frac{\partial T_p}{\partial z}\right|_{z=0} = h_b \left(T_R - T_p\big|_{z=0}\right),$$
$$\alpha_p \left.\frac{\partial T_p}{\partial r}\right|_{r=R} = h_r \left(T_R - T_p\big|_{r=R}\right),$$
$$\left.\frac{\partial T_p}{\partial r}\right|_{r=0} = 0,$$

where the Dirichlet condition at the right boundary has been approximated, for convenience, as a Robin boundary condition with a large transfer coefficient h_r.

In the POD method, the product temperature is approximated by truncated Fourier series expansion of the form:

$$T_p(r,z,t) \approx \sum_{i=1}^{n} \phi_i(r,z) s_i(t), \tag{23}$$

where n is the number of elements required to obtain a sufficiently accurate approximation. The set of modes $\{s_i(t)\}_{i=1}^{N}$ contain the spatial information of the solution whereas the basis function set $\{\phi_i(r,z)\}_{i=1}^{N}$ contains the spatial information and they are obtained by solving the following eigenvalue problem:

$$\lambda_i \phi_i = \int_{\mathcal{V}} \mathcal{K} \phi_i \mathrm{d}\mathcal{V},$$

where the kernel $\mathcal{K}$ is computed as:

$$\mathcal{K} = \frac{1}{p} \sum_{i=1}^{p} T_{p,i} T_{p,i}^{'},$$

with $T_{p,i} \in \mathbb{R}^N$ being vector of food product temperature measurements at different N spatial points and at time t_i. The prime symbol indicates the transpose. The basis functions obtained in this way are orthonormal, i.e:

$$\int_{\mathcal{V}} \phi_i \phi_j \mathrm{d}\mathcal{V} = \begin{cases} 1 & \text{if} \quad i = j \\ 0 & \text{if} \quad i \neq j \end{cases}.$$

Now, the Fourier equation (22) is projected over the basis set to obtain the set of modes $\{s_i(t)\}_{i=1}^{N}$. In practice, such projection is performed by multiplying Eq. (22) by the basis functions and integrating over the spatial domain, i.e.

$$\int_{\mathcal{V}} \phi_j \frac{\partial T}{\partial t} \mathrm{d}\mathcal{V} = \alpha \int_{\mathcal{V}} \phi_j \mathcal{A} T \mathrm{d}\mathcal{V}; \qquad j = 1, ..., n,$$

where $\mathcal{A}$ represents the Laplacian operator in cylindrical coordinates. Substituting T_p by the series expansion (23) and using the boundary conditions, the following set of ODEs is obtained:

$$\frac{\mathrm{d}s}{\mathrm{d}t} = \left(\alpha_p A_{\alpha_p} + h_t A_{h_t} + h_b A_{h_b} + h_r A_{h_r}\right) s + \left(h_t B_{h_t} + h_b B_{h_b} + h_r B_{h_r}\right) T_R, \tag{24}$$

where $s = [s_1, s_2, ..., s_n]^T$. Each element (i, j) of A_{α_p}, A_{h_t}, A_{h_b} and A_{h_r} is computed as:

$$A_{\alpha_p}(i,j) = -\int_{\mathcal{V}} \boldsymbol{\nabla}\phi_i \boldsymbol{\nabla}\phi_j \, \mathrm{d}\mathcal{V},$$

$$A_{\ell}(i,j) = -\int_{\mathcal{B}_\ell} \phi_i \phi_j \, \mathrm{d}\mathcal{B}\ell; \qquad \text{with } \ell = h_t, h_b, h_r,$$

whereas vectors B_{h_t}, B_{h_b} and B_{h_r} is obtained as:

$$B_{\ell}(i) = \int_{\mathcal{B}_\ell} \phi_i T_r \, \mathrm{d}\mathcal{B}_\ell; \qquad \text{with } \ell = h_t, h_b, h_r,$$

with $\mathcal{B}_{h_t}$, $\mathcal{B}_{h_b}$ and $\mathcal{B}_{h_r}$ being, respectively, the top, bottom and right boundaries.